Toxicology Research

Accepted Manuscript

ROYAL SOCIETY OF CHEMISTRY

www.rsc.org/toxicology

Rescue of cells from apoptosis increases DNA repair in UVB exposed cells: implications for the DNA damage response

Mahsa Karbaschi[1#], Salvador Macip[2], Vilas Mistry[3], Hussein H. K. Abbas[3], George J. Delinassios[4], Mark D. Evans[5], Antony R. Young[4] and Marcus S. Cooke[1]

Running title: Rescue from apoptosis increases DNA repair

[1]Dept. Environmental and Occupational Health, Robert Stempel College of Public Health and Social Work, Florida International University, 11200 S.W. 8th Street, Miami, FL 33199

[2]Dept. Biochemistry, Henry Wellcome Building, University of Leicester, Leicester, LE1 9HN

[3]Oxidative Stress Group, RKCSB, University of Leicester, Leicester, LE2 7LX, UK.

[4]King's College London, St John's Institute of Dermatology, 9th Floor, Tower Wing, Guy's Hospital; Great Maze Pond, London SE1 9RT, UK.

[5]School of Allied Health Sciences, Faculty of Health and Life Sciences, De Montfort University, The Gateway, Leicester, LE1 9HB, UK

[#] To whom correspondence should be addressed:

Mahsa Karbaschi,

Room 347, AHC 5, Dept. Environmental & Occupational Health, Florida International University, 11200 S.W. 8th Street, Miami, FL 33199. E-mail: mahsa.karbaschi@fiu.edu. Phone 1-305-348-4076

ABSTRACT

Classically, the nucleotide excision repair (NER) of cyclobutane pyrimidine dimers (CPD) is a lengthy process ($t_{1/2}$ > 48 h). Using the T4 endonuclease V-modified comet assay, we uniquely found a far more rapid repair of UVA-induced CPD ($t_{1/2}$ = 4.5 h) in human skin keratinocytes. The repair of UVB-induced CPD began to slow within 1 h of irradiation, causing damage to persist for over 36 h. A similar trend was noted for the repair of oxidatively-modified purine nucleobases. Supportive of this differential repair, we noted an up-regulation of key genes associated with NER in UVA-irradiated cells, whereas the same genes were down regulated in UVB-irradiated cells. There were no significant differences in cell viability between the two treatments over the first 6 h post-irradiation, but after 24 h apoptosis had increased significantly in the UVB-irradiated cells. The role of apoptosis was confirmed using a pan-caspase inhibitor, which increased CPD repair, similar to that seen with UVA. These data indicate that the cellular 'decision' for apoptosis/DNA repair occurs far earlier than previously understood, and that the induction of apoptosis leads to lesion persistence, and not vice versa. This also highlights a new, potential increased carcinogenic risk from UVA-induced DNA damage as, rather than undergoing apoptosis, high levels of damage are tolerated and repaired, with the attendant risk of mutation.

INTRODUCTION

Skin cancer has a high incidence in countries with large populations of white skinned individuals, including the UK, USA and Australia, and the incidence continues to rise, with UVR the principal aetiological agent in most cases (1, 2). Skin type, hair and eye colour are predictive of skin cancer risk, implying protection by constitutive melanin, and greater DNA repair may contribute (3). UVR is a complete carcinogen, both initiating the DNA damage that can lead to mutagenesis, and promoting carcinogenesis, for example via immunosuppression (1, 2), with consequential mortality (in the case of melanoma) and morbidity (non-melanoma skin cancer). Whilst UVB (280-320 nm) constitutes a maximum of 5% of the UVR reaching the earth's surface, it is widely considered the most mutagenic and carcinogenic component (4). This is largely due to its ability to damage DNA, which directly absorbs UVB, causing dimerisation of adjacent pyrimidine nucleobases and forming cyclobutane pyrimidine dimers (CPD) and pyrimidine (6-4) pyrimidone photoproducts (6-4)PP (5). Direct evidence for the involvement of these lesions in carcinogenesis derives from the significant number of *p53* mutations (TC → TT and CC → TT) detected at bipyrimidine sites in skin cancers. The remaining 95% of solar UVR reaching the earth's surface is UVA (320-400 nm). Traditionally, there has been less concern over the contribution from UVA to skin carcinogenesis, compared to UVB, not least because UVA is extremely poorly absorbed by DNA, and hence unlikely to damage DNA directly. As a result, until relatively recently sunscreens provided predominantly UVB protection, unwittingly leading to greater exposure to UVA (6). The popularity of high intensity UVA sources in artificial tanning salons has been proposed as a route to a 'safe tan', again contributing to greater exposure. However, UVA can damage DNA via the induction of oxidative stress, leading to products such as 8-oxo-7,8-dihydro-2'-deoxyguanosine (8-oxodG) (7). Whilst such damage may have profound consequences for the cell (8), the failure to match the UVA mutation spectrum to that which

would be expected for 8-oxodG (a predominance of G:C to T:A transversions) (9, 10) has led to the suggestion that oxidative stress, and oxidatively damaged DNA specifically, contributes to post-initiation events in UVR-induced carcinogenesis, for example promotion (5) and immunosuppression (11).

There are a growing number of studies which have reported the induction of CPD [T<>T, >> T<>C > C<>T (12)] by UVA (13-16) in bacteria (17), mammalian cells and skin (7, 18-21), via a mechanism proposed to be independent of a cellular photosensitiser i.e. direct absorption (22, 23). Nucleotide excision repair (NER) is a major DNA repair system, in all species, and the sole mechanism for bulky adducts (24) such as CPD and (6-4)PP (25). NER operates via two distinct pathways: global genome repair (GGR), for removal of lesions from the overall genome; and transcription-coupled repair (TCR) that targets transcribed sequences of actively expressing genes (reviewed in (26-28)). It is well established that the repair of (6-4)PP is far more effective than the repair of CPD (29-32), with the majority of (6-4)PP being removed within 10-12 h (18), whereas >50 % of CPD persist for longer than 48 h (12), suggesting a degree of resistance to repair (33). Indeed, there is a degree of differential repair between the different forms of CPD, following UVB irradiation, with T<>T being the slowest, followed by C<>C and T<>C equally, and C<>T being the fastest (34). Lesion structure, and hence distortion of the DNA duplex, sequence context and cellular concentration of DNA damage-sensing proteins, such as XPC and DDB2, have all been suggested as explanations for these differences in repair rates (34). It is therefore a combination of this resistance to repair, propensity for formation, by both UVB and UVA, and mutagenicity which gives T<>T a major role in UVR-induced carcinogenesis. Furthermore, a few early reports have suggested that the repair of UVA-induced T<>T is significantly slower than UVB-induced T<>T (12, 35), or even absent in the basal layer of the epidermis (16). Such data emphasise further the importance of T<>T, and the health risks

posed by UVA. In an effort to understand better why the same lesion is repaired at different rates, when induced by different wavelengths, we sought to investigate these findings in well established, *in vitro* human skin cell line models.

MATERIALS AND METHODS

DNA repair enzymes T4 endonuclease V (T4endoV), human 8-oxoguanine DNA glycosylase 1 (hOGG1) and endonuclease III (endoIII), were purchased from New England-Biolabs (Hitchin, UK). H_2O_2 was obtained from Sigma-Aldrich (Dorset, UK). The pan-caspase inhibitor, Z-VAD-FMK was obtained from Promega (Madison, WI, USA).

Cell lines and culture conditions. The human keratinocyte cell line, Human adult low Calcium high Temperature (HaCaT), was a kind gift from Professor N.E. Fusenig (Deutsches Krebsforschungszentrum, Heidelberg, Germany (36). This cell line reveals a heteroploid stemline with specific stable marker chromosomes, but is not tumourigenic (36). Cells at passage number 50 were grown as a mono-layer in Nunclon culture flasks at 37 °C in a 5% CO_2 humidified incubator and in medium comprised of 1:1 DMEM/Hams F12 medium supplemented with 10% (v/v) fetal bovine serum, 1 mM sodium pyruvate and 2 mM Glutamax. Primary adult, human dermal fibroblasts (HDF), isolated from adult skin, were obtained from Invitrogen (Paisley, UK). HDFs were grown as a mono-layer in Nunclon culture flasks at 37 °C in a 5% CO_2 humidified incubator in fresh medium 106 (a liquid medium for the culture of human dermal fibroblasts; Invitrogen, UK) supplemented with low serum growth supplement. All cell culture materials were purchased from Invitrogen, Paisley, UK.

Cell treatments and post-irradiation manipulation. UVA (with a peak spectral emission at 355 nm) and UVB (with a peak spectral emission at 310 nm) irradiations were performed using a custom made exposure cabinet (Hybec Ltd., Leicester, UK), which contains a bank of six Philips Cleo Performance/40W fluorescent tubes, with a Schitt Desag M-UG2 UVR transmitting absorption glass filter (HV Skan, Solihull, UK) to remove both visible and infrared wavelengths, and six Ultraviolet-B TL20W/01 (TL01) fluorescent lamps (Philips) which were closely spaced. The wavelength emission spectra of the lamps

(including the filtering) were characterised using a single monochromator diode array spectroradiometer, as previously reported [37], together with a Bentham Spectral radiometer (Bentham Instruments Ltd, Reading, UK). Spectral analysis confirmed that Cleo Performance lamps emit a broadband UVA spectrum (99.6% UVA, 0.4% UVB) and visible light contamination was efficiently removed by the M-UG2 glass filter (Figure 1 A). This very small, longer wavelength UVB (~315-320 nm) contamination in our UVA source is unlikely to have a significant biological effect. Spectral analysis demonstrated that the UVB lamps were predominantly UVB (85.9 % UVB, 14.1% UVA; Figure 1 B). The UVR intensity was measured using a UVX Radiometer (Ultra Violet Products, Upland, USA, distributed by Fisher Scientific, Loughborough, UK) in conjunction with a UVX-36 sensor for UVA and a UVX-31 sensor for UVB (Ultra Violet Products, Upland, USA) prior to UVR exposure.

Sub-confluent HaCaT and HDF cells (n = 30,000 for comet assay; n = 2 x 10^5 flow cytometry; n = 2 x 10^6 for RNA extraction) were irradiated in suspension in PBS, in a petri dish or six well plate with no lid, on ice with 10 J/cm^2 UVA or 1 J/cm^2 UVB. Control samples were sham-irradiated (cells were irradiated whilst covered with aluminium foil). Following irradiation, and prior to various investigations, cells were left in complete medium to repair for different time points (0 min, 30 min, 1 h, 6 h, 12 h, 24 h and 36 h) at 37 °C in 5% CO_2, humidified incubator. At each time point, the adherent cells were trypsinised and used in subsequent assays for DNA damage and repair, viability and gene expression (see below).

For the treatment of HaCaTs with H_2O_2, cells were seeded in 12 well plates (Greiner Bio-One GmbH, Frickenhausen, Germany) and incubated overnight. After removing the medium, the cells were washed with PBS, and then exposed to freshly prepared H_2O_2 (100 μM, final concentration) for 30 min on ice. After exposure, the H_2O_2 was removed by washing with PBS, medium reintroduced and the cells returned to the incubator and allowed to repair for

varying timepoints (0 min, 1 h, 3 h, 6 h, and 24 h) prior to analysis by hOGG1- and endoIII-modified comet assay (see below).

Where indicated, HaCaTs were treated with various concentrations (0 – 300 μM) of the caspase inhibitor Z-VAD-FMK. Treatment comprised incubation of cells with Z-VAD-fmk for both 24 h before and 24 h after UVR exposure (inhibitor-containing medium was removed, and irradiation performed with cells suspended in PBS, as described above). After irradiation, cells were returned to the incubator and 24 h allowed for potential repair, prior to analysis by T4endoV modified comet assay.

T4 endonuclease V modified alkaline comet assay. DNA damage was assessed using T4endoV modified alkaline comet assay which recognises cyclobutane pyrimidine dimers. Whilst there are no specific data concerning preferential activity towards the potential combinations of pyrimidines in CPD, inferences can be made from the ability of the enzyme to incise at all combinations of CPD, in plasmids and small bacteriophage vectors, suggesting all are equal substrates. Furthermore, the predominant form of CPD induced by UVA and by UVB is T<>T (12). It has been reported that T4endoV also removes 4,6-diamino-5-formamidopyrimdine (FapyAde) (38), a hydroxyl radical induced product of adenine, and that this is induced by both UVC and UVB (39). However, with a level of activity (1-3% of its activity towards CPD) that the authors conclude may not be biologically relevant in vivo (38). This finding is entirely consistent with our studies with T4endoV modified comet assay and cells exposed to ionising radiation (data not shown). On this basis, and under our conditions, we conclude that there will be minimal contribution from FapyAde to the measurement of CPD by the T4endoV modified comet assay. UVR may also generate the formation of AP sites, which may be detected by the AP lyase activity of T4endoV, which could lead to an overestimation of CPD. However, it is possible to discriminate between AP sites and T<>T by plotting data derived from the alkaline comet assay alone (which

representing all frank strand breaks and those induced by the action of high pH on AP and other alkali-labile sites) versus in conjunction with the T4endoV (which includes all of the former strand breaks, plus those induced by the enzyme). This is a well established approach to determine levels of strand breaks and alkali-labile sites (which includes AP sites).

The T4endoV modified comet method was performed as described previously (37, 40) with specific refinements of the assay for HaCaTs and HDFs. Both the concentration of, and incubation period for, T4endoV were optimised at 0.1 U/μL and 60 min for HaCaTs and 0.02 U/μL plus 60 min for HDFs, at 37 °C in a humidified atmosphere. The remainder of the comet assay protocol was as described below.

Human 8-oxoguanine DNA glycosylase 1-modified comet assay. DNA damage was assessed using hOGG1-modified comet assay, as described previously (37, 40) with specific refinements of the assay for HaCaTs and HDFs. hOGG1 recognises 8-oxo-7,8-dihydroguanine (8-oxoGua) and 8-oxo-7,8-dihydrodenine, but also two other hydroxyl radical-induced products, 2,6-diamino-4-hydroxy-formamidopyrimidine (FapyGua) (41) and, to a much lesser extent, FapyAde (42). For both HaCaTs and HDFs the concentration of, and incubation period for, hOGG1 were optimised at 3.2 U/mL and 45 min, at 37 °C in a humidified atmosphere.

Endonuclease III-modified comet assay. DNA damage was assessed using an endo III-modification of the previously described alkaline comet assay (37, 40)), with specific refinements of the assay for HaCaTs. Both the concentration of and incubation period for endoIII were optimised at 10 U/mL and 45 min, at 37 °C in a humidified atmosphere. Endo III recognises a number of free radical-induced DNA products, which are exclusively pyrimidine-derived (e.g. thymine glycol, uracil glycol, 5-hydroxycytosine and 5-hydroxyuracil) (43), with the exception of FapyAde (44).

General comet assay protocol. At each analysis time point, 3 x 10^4 cells from each treatment were centrifuged at 400 x g for 4 min, then suspended in 200 μL of 0.6% low melting point agarose. 80 μL of agarose, containing approximately 12,000 cells, were dispensed onto glass microscope slides, pre-coated with 1% normal melting point agarose. The agarose was allowed to set on ice under a 22 x 22 mm cover slip (VWR International, distributed by Fisher Scientific, Loughborough, UK). The cover slips were then removed carefully, and the slides incubated overnight at 4 °C in lysis buffer (2.5 M NaCl, 10 mM Tris–HCl, 100 mM disodium EDTA, pH 10 and 1% Triton X-100). On the following day, the slides were washed once with double distilled water, and the cells then incubated with appropriate enzyme under 22 x 22 mm cover slips (using the above optimised conditions). After the incubation period, cover slips were removed and the slides placed in a cold (4 °C) electrophoresis tank, filled with cold alkaline electrophoresis buffer (double distilled water, 300 mM NaOH, 1 mM disodium EDTA, pH ≥ 13), for 20 min and then underwent electrophoresis at 27 V and 300 mA for 20 min. Slides were neutralised with 0.4 M Tris–base, pH 7.5 for 20 min, followed by washing with double distilled water, and then left to dry at room temperature, in the dark, overnight. On the third day, prior to staining, slides were re-hydrated with double distilled water for 30 min, and then covered with 2.5 μg/mL propidium iodide solution (diluted in double distilled water) for 15-20 min. Afterwards, the slides were washed again for another 30 min at room temperature in dark and allowed to dry. All procedures were carried out under red light to decrease the potential formation of artefactual DNA damage. Comets were visualised by using a combination of an on-line CCD camera, fluorescence microscopy at ×20 magnification, and Comet Assay IV software version 4.2 (Perceptive Instruments, Suffolk, UK). 50 cells per gel (100 cells in duplicate slides) were scored and the percentage of tail DNA in each comet was calculated for each nucleoid image (45).

Cell Viability. Human Annexin V-FITC Apoptosis Kit (Bender Medsystems, Vienna, Austria) was used to assess viability of HaCaTs and HDFs at the indicated post-irradiation time points. The cells (2 x 10^5 cells) were trypsinised and centrifuged at 300 × g for 5 min, prior to resuspension in 5 mL of fresh media and incubated at 37 ºC for another 30 min. Cells were then transferred to FACS tubes and centrifuged at 300 × g for 5 min. The supernatant was discarded and the pellet was resuspended in 1 mL of Annexin buffer, followed by the addition of 4 µL of Annexin V-FITC conjugate and incubation at room temperature for 10 min. Subsequently, 30 µL (0.05 mg/mL) propidium iodide were added and incubated at room temperature for 1 min. Finally, the cells (n=10,000 per treatment) were analysed by flow cytometry (FACScan flow cytometer, Becton Dickinson, Oxford, UK) using CellQuest software (Becton Dickinson, San Jose, CA).

RNA extraction. After irradiation, the HaCaTs were returned to the incubator in fresh medium, and allowed to repair for 0 h, 6 h and 24 h, after which the cells were frozen in DMEM containing 5% DMSO, until analysis. Total RNA was extracted from the frozen cells using Allprep DNA/RNA/Protein Mini Kit (Qiagen, UK). RNA concentration was determined by Nanodrop (Thermo Scientific, UK, distributed by Labtech International Ltd, Ringmer, UK).

Expression of genes associated with NER. Primer sequences were designed using Primer 3 software (46) and the specificity of the primers tested using NCBI primer blast tools (http://www.ncbi.nlm.nih.gov/tools/primer-blast/index.cgi?LINK_LOC=BlastHome). The predicted amplification product was then examined for possible primer secondary structures and for duplex formation, by testing on DNA mfold (http://frontend.bioinfo.rpi.edu/applications/mfold/cgi-bin/dna-form1.cgi) and Vector NTI (64) software. The forward and reverse oligonucleotide sequences were 5'-TGTGATTGCCTTCTTACAACAGAG-3' and 5'-TAGGGTTTGCCTTGGTATCTTG-3'

for XPA; 5'-CTGCCATCCTTGGGTATTGTCGT-3' and 5'-GCCTCACCACTCTTGCTTTCTTCAG-3' for XPC; 5'-CTAAGATGTGTATCCTGGCCGACT-3 and 5'-AAGTCCTGCTCTAGCTTCTCCATC -3' for ERCC1; 5'-ATGGGGAAGGTGAAGGTCG-3' and 5'-GGGGTCATTGATGGCAACAATATC -3' for GAPDH.

Two µg of isolated RNA were reverse transcribed into double-stranded cDNA with a mixture of random primers and oligo(dT) primer using the cDNA synthesis Kit (Cedar Creek, TX). Real-time PCR was performed on a MX4000 spectrofluorometric thermal cycler (Stratagene, Amsterdam, The Netherlands) as described elsewhere (47). The amplification protocol consisted of a denaturation step at 95 °C for 4 min and 50 cycles of 95 °C for 30s, 69 °C for 1 min, and 72 °C for 30 s. Serial dilutions of a cDNA sample were amplified to generate standard curves of amplification for each gene of interest, confirming the linear relationship between the threshold cycle and the log (RNA input). The quantity of each transcript was determined against the respective standard curve and normalised against both expression of the corresponding NER gene immediately after irradiation, and expression in control sham irradiated samples, according to Plaffl (2008) (48).

Protein extraction and Western blotting. After appropriate treatment, cells were lysed by the addition of Laemmli buffer (2% SDS, 10% glycerol, 50mM Tris pH6.8), and the resulting lysates heated to 94 °C for 5 min before sonication. The samples were then vortexed, centrifuged for 1 min at 16,000 x g and then the protein concentration determined using a Pierce BCA Protein Assay Kit (Thermo Scientific, Cramlington, UK), according to the manufacturer's instructions. The protein samples were loaded onto 4-10% gradient SDS-PAGE gels and transferred to PVDF membrane (Immobilon–P, Millipore, Watford, UK). Once transferred, the membrane was blocked TBS-T-milk [50 mM Tris pH 7.65, 150 mM NaCl, 0.1% (v/v) Tween-20, 5% (w/v) fat free milk powder]. The membrane was incubated

with the primary antibody (Cell Signalling Technology, Berverly, MA, USA), diluted in TBS-T-BSA [50 mM Tris pH 7.65, 150 mM NaCl, 0.1% (v/v) Tween-20, 5% BSA], then washed thoroughly with TBS-T. The membrane was then incubated with the HRP-labelled secondary antibody (Abcam, Cambridge, UK; diluted 1:5000 in TBS-T-milk), prior to washing thoroughly. Bands were visualised with ECL Western Blotting Substrate (#32106, Thermo Scientific, Rockford, USA) according to manufacturer's instructions.

Statistical analysis. Statistical analyses were performed using GraphPad Prism, version 6.02 (GraphPad, CA, USA). For all variants of Comet assay, the data were evaluated using non-parametric tests (Mann Whitney) to compare the values between two or more groups. The level of statistical significance was set at $p < 0.05$.

RESULTS

Induction of DNA damage in human skin cells exposed to UVR. Following optimisation of the T4endoV-modified comet assay for HaCaTs, this assay demonstrated that irradiation of HaCaTs with 10 J/cm^2 UVA or 1 J/cm^2 UVB lead to the induction of significant ($P < 0.0001$) levels of CPD over control, sham irradiated cells (Figure 2 A and B). Performing comet analysis in the absence of T4endoV allows for the examination of strand breaks (SB) and, at pH >13, alkali-labile sites (ALS), which may include apurinic/apyrimidinic (AP) sites, oxidised AP sites and certain modified nucleobases (49)depending upon the DNA damaging system used. We also noted the formation of significant and comparable levels of SB/ALS following both treatments, compared to control, sham irradiated cells (Figure 2 A and B).

Faster repair of UVA- versus UVB-induced CPD in human skin cells. Following irradiation with the above doses of UVR, we monitored levels of CPD in nuclear DNA of HaCaTs over a 36 h time period. Soon after irradiation, the repair of rate of UVB-induced CPD decreased dramatically, with a large amount (38%) of damage still remaining after 36 h (Figure 3 A). This overall slow repair rate is consistent with observations reported by others in human skin [e.g. (12, 50, 51)] and cultured cells [e.g. (34, 35)] with a $t_{1/2} > 48$ h, which is widely regarded to be characteristic of T<>T specifically. For the UVA-irradiated cells, we again noted an initial period of rapid repair (the first ~6 h) similar to that seen for UVB-induced CPD (Figure 3 A). However, in contrast to the UVB-irradiated cells, this faster rate of repair was maintained over the subsequent 30 h, with levels of CPD returning to approximately baseline (8% damage remaining) at ~24 h (Figure 3 A) and a $t_{1/2}$ of 4.5 h. The divergence in the rate of repair between UVA- and UVB-induced CPD began as early as 1 h post-irradiation (Figure 3 A inset). As this observation was in contrast to two earlier reports which described the repair of UVA-induced CPD to be slower than UVB-induced CPD (12, 35), we considered it possible to have been unique to HaCaTs. We therefore repeated the

above experiment using HDFs, a primary fibroblast culture, to address any potential issues which may be associated with using a spontaneously transformed cell line (36). Experiments with HDFs showed the same pattern of results we noted with HaCaTs, with the repair of UVA-induced CPD considerably faster than that for UVB-induced CPD, which again showed the characteristic pattern of a large amount of T<>T (54%) remaining after 36 h (Figure 3 B). As noted elsewhere (34, 52), we observed slightly faster repair of UVB-induced CPD in keratinocytes, compared to fibroblasts and, uniquely to our study, this also applied to UVA-induced CPD (Figure 3 A and B). To demonstrate that the T4endoV modified Comet assay has sufficient dynamic range to accurately report the levels of damage noted, we performed a dose-response study. This showed that the number of CPD increased linearly with dose of UVR (Figure 3 C). It is possible that UVR dose, and hence induced levels of damage, affects the rate of repair, although in our experiments levels of damage induced by 10 J/cm^2 UVA and 1 J/cm^2 UVB were comparable (Figure 2). To test this we examined the rate of CPD removal following increasing doses of UVB (0.2-1.0 J/cm^2), and showed that initial levels of damage had little effect on the rate of repair, over the dose range used (Figure 3 D).

Induced levels of CPD were lower in HDFs, compared to HaCaTs, following the same dose of either UVB or UVA (Figure 4 A and B). This is contrary to an earlier report, which indicated the yield of T<>T and T<>C, specifically, to be higher in primary fibroblasts than primary keratinocytes following UVB irradiation (34). Whilst this was also the case for UVA-induced SB/ALS (Figure 4 A), there was no difference in levels of SB/ALS between HaCaTs and HDFs, following UVB irradiation (Figure 4 B). To better understand our observation of differential CPD repair, we also examined the repair of SB/ALS, noting it to be far more rapid than CPD, reaching approximate baseline levels within 24 h, in both HaCaTs and HDFs (Figure 4 C and D, respectively). Curiously, the repair of UVA-induced

SB/ALS in HDFs was initially faster than that following UVB (Figure 4 D), approaching baseline levels slightly sooner than that following UVB.

Faster repair of UVA- versus UVB-induced oxidised purines. In order to further test the observed differential effect of UVA- and UVB-irradiation on DNA repair, we examined the removal of 8-oxoGua, which is predominantly repaired by base excision repair, a process distinct from NER. Using the hOGG1-modified comet assay, we noted induced levels of 8-oxoGua in HaCaTs, to be significantly greater ($P<0.001$) following 10 J/cm^2 UVA (~30 % tail DNA), compared to 1 J/cm^2 UVB (~25 % tail DNA) (Figure 5 A). The hOGG1-modified comet assay was also used to assess repair, and we again noted that, after an initial period of moderate repair, the rate of 8-oxoGua repair slowed in the UVB-irradiated cells, but remained more rapid in the UVA-irradiated cells, an observation reproduced in both HaCaTs (Figure 5 B) and HDFs (Figure 5 C).

To confirm the BER rate of 8-oxoGua in HaCaTs, we determined the kinetics of lesion loss following H_2O_2 treatment, as a 'classical' inducer of 8-oxoGua, using the hOGG1-modified comet assay (Figure 5 B). This showed that repair of H_2O_2-induced 8-oxoGua was similar to that of UVA-induced 8-oxoGua in both HaCaTs and HDFs (Fig 4B and C, respectively), approaching baseline at 24 h. This finding was further supported by examining the removal of oxidised pyrimidines in HaCaTs, again induced by H_2O_2, by following their BER using the endoIII-modified comet assay (Figure 5 B)

UVB irradiation-induced apoptosis is accompanied by a down-regulation of key NER genes. To evaluate the effects of UVR exposure on cell viability, and therefore potential to undertake DNA repair, we examined HaCaTs for Annexin V staining, as an early indicator of apoptosis, at several timepoints post-irradiation. Baseline levels of viability were 91%. One hour following irradiation with UVA, this decreased to 77%, and remained at 79% at six and 24 h post-irradiation (Figure 6 A). A similar pattern was seen for UVB irradiated

cells, with viability of 83% and 84% at one and six hours post-irradiation. However levels of viable cells decreased dramatically to 43%, with a corresponding significant increase in apoptosis at 24 h (Figure 6 B). This result was, to some extent, reproduced in HDFs, although these cells were demonstrated to be much more sensitive to both UVB- and UVA-induced apoptosis than HaCaTs (Figure 6 C and D). Indeed, this finding might explain the slower repair kinetics of UVA-induced CPD in HDFs (Figure 3 B) compared to HaCaTs (Figure 3 A).

Concurrent with the pattern of time-dependent increase in apoptosis following UVB irradiation seen in Figure 5 B, we noted significant, time-dependent decreases in the expression of key NER genes (XPA, XPC and ERCC1; Figure 6 E). In contrast, for UVA, following an initial small immediate decrease, expression of all three NER genes recovered to baseline levels within 24 h (Figure 6 E). This sustained down regulation of NER gene expression seems likely to account for the slower repair of UVB- versus UVA-induced CPD.

Inhibition of UVB-induced apoptosis restores DNA repair. It appeared that DNA repair and the induction of apoptosis might be linked mechanistically. Therefore, to confirm that UVB-induced apoptosis contributes to an overall decrease in DNA repair, as measured by Comet assay, we investigated whether inhibition of apoptosis modulated levels of damage. We noted a dose-responsive decrease in CPD levels, determined by T4endoV-modified comet assay, 24 h post-UVB irradiation (Figure 7 A), following treatment of HaCaTs with increasing concentrations of pan-caspase inhibitor Z-VAD-FMK. This clearly indicated that inhibition of apoptosis increased DNA repair activity. As expected, cleavage of downstream factors in the apoptotic cascade e.g. caspase-3, was prevented by Z-VAD-FMK treatment (Figure 7 B), together with increasing the number of viable cells following UVB irradiation (Figure 7 C).

Taken together these data indicate CPD are more rapidly repaired than reported previously, consistent with their potential mutagenicity and the importance for the cell to exclude them from DNA. However, the induction of apoptosis in UVB irradiated cells results in the slow repair of CPD, together with oxidised purines. Furthermore, the induction of apoptosis appears to be independent of the levels of damage generated by irradiation, suggesting some other factor is the trigger for apoptosis in UVB irradiated cells.

DISCUSSION

This is the first report of the differential repair, and description of the underlying mechanism, of UVA- versus UVB-induced CPD and oxidatively damaged purines. This adds to a small but growing number of reports which describe differential cellular responses to UVA and UVB irradiation. For example, UVA is associated with conferring greater resistance to the induction of apoptosis (53); UVA-induced, oxidatively generated purine damage is repaired faster than UVB-induced CPD (33); UVB irradiation results in more effective cell cycle arrest, compared to UVA (54). Our results demonstrate profound and fundamental differences in the cellular response to UVA and UVB, which are independent of cell type, and confirm that there are wavelength-dependant differences in the cellular response to damage.

It is conceivable, however unlikely, that subtle differences in experimental design could contribute to the results seen here. These include: spectral characteristics of UVR source, damage/repair detection methodology; doses of UVR used and cell type. The majority of prior studies have only reported the peak emission wavelengths, and not described the exact emission spectrum, making comparison with our UVR sources difficult. However, our peak emission wavelengths for UVA and UVB are entirely consistent with those reported previously. In order to demonstrate that the T4endoV-modified comet assay is appropriate for the study of CPD induction and repair, we compared our rate of UVB-induced CPD with that reported in the literature. There would appear to be broad agreement that the repair rate of T<>T, induced by solar simulated radiation, leads to ~ 70 % T<>T remaining at 6 h, ~50 % T<>T remaining at 24 h (51, 55-57), and ~40-47% remaining at 48 h, post-exposure (55, 58, 59), using a variety of methods (immunoassay, DNA nicking assay and ^{32}P-postlabelling). Values, derived using HPLC-MS/MS, tend to be higher (80% and 70% T<>T remaining after 24 and 48 h respectively), but similarly indicate a protracted time course of

lesion removal (12, 34, 35), which has become recognised as characteristic of CPD. Taken together, these values are entirely consistent with our data for the repair of UVB-induced T<>T, indicating that the T4endoV-modified comet assay is suitable for the study of CPD induction and repair. It is possible that the induced level of T<>T, prior to repair, may somehow influence the subsequent rate of repair, for example, as a consequence of an excess of substrate. In the studies where the repair of UVA-induced T<>T was reported to be slower than that for UVB-induced T<>T, initial damage levels were 4.0 T<>T/10^6 normal bases (induced by UVA), with 20.0 T<>T/10^6 normal bases (induced by UVB), a five-fold difference in damage (34); and ~4.0 T<>T/10^6 normal bases (induced by UVA), compared to ~4.6 T<>T/10^6 normal bases (induced by UVB) (35). This indicates that the initial damage level does not influence the rate of repair. In the present study, we examined the repair of 50 %TD (induced by UVA), with 65 %TD (induced by UVB), clearly more comparable levels of lesion. However, on the basis of the literature it would appear that, if at all, higher levels of T<>T leads to their faster repair (50).

Given the 'classical' understanding that the NER of CPD is slow, compared to the NER of (6-4)PP or BER of oxidised purines and pyrimidines (33), the faster repair of UVA- versus UVB-induced DNA damage, and CPD in particular, represents new and, perhaps surprising, information. To the best of our knowledge, the only other description of the repair kinetics of UVA-induced CPD are two reports from Douki's group (12, 35). In both articles, the authors note the apparent slower repair of UVA-induced CPD (T<>T, specifically), compared to UVB-induced T<>T, in contrast to our findings. Collectively, these results suggest an intrinsic difference in how UVA-induced CPD/T<>T are processed by the cell, perhaps related to the mechanism by which they are formed. Indeed, it has been suggested that their mechanism of formation differs, UVB-induced CPD being generated from direct

absorption by DNA (4), and UVA-induced CPD being formed indirectly via a photosensitisation reaction; although this has been challenged recently (22).

The basis for this differential rate of repair appears to relate to the cellular response to UVA or UVB irradiation. The initial rate of CPD repair is equally rapid, irrespective of whether induced by UVA or UVB, consistent with the activation of the DNA damage response (DDR). However, one hour post-irradiation a difference in the rate of repair begins to become apparent. The expression of NER genes shows a down regulation following both UVA and UVB irradiation, which would lead to a decrease in *de novo* synthesis of repair proteins, and limiting the effectiveness of the DNA repair response. However, unlike the expression of NER genes in UVB irradiated cells, whose down regulation continued to increase with time, UVA irradiated cells produce a markedly more rapid recovery in expression, returning to baseline levels of expression within 24 h, which is entirely consistent with the faster repair of CPD.

Our data show clearly that the slower NER of UVB-induced CPD, and indeed BER of UVB-induced oxidatively damaged DNA, is due to the induction of apoptosis, and that rescuing cells from apoptosis allows repair to occur. The conclusion is that UVB-induced apoptosis significantly attenuates, but does not entirely inhibit, repair. Indeed it has been suggested that single- and double-strand breaks (not necessarily induced by apoptosis) can lead to the impairment of NER (60). The link between apoptosis and DNA repair is not entirely clear. Our data show that the early induction of apoptosis causes repair to slow. However the prevailing view appears to be that (i) DNA repair is the determinant for whether or not apoptosis is induced, for example the efficient repair of CPD leads to the avoidance of apoptosis (61, 62) and NER-deficient cells being extremely sensitive to UVR-induced cell death [reviewed in (63)]; and (ii) a period of ~ 24 h is required for the cell to determine whether or not sufficient DNA repair can occur to prevent apoptosis (64). In contrast to the

above, we propose that there is an early trigger for apoptosis which occurs shortly after UVB irradiation, and has the effect of slowing repair which is evident within one hour. Supportive of this, expression of NER genes is down-regulated (and remains down-regulated), soon after UVB irradiation. Despite this, and consistent with other studies, levels of apoptosis do not become significant until 24 h post-irradiation, despite using Annexin V, which is a sensitive, early marker of apoptosis. This would appear to have a more methodological, rather than biological basis, as apoptosis is a process which requires time to become evident. Simply because significant levels cannot be measured soon after irradiation does not demonstrate the process has not begun.

Taken together these data indicate that the cellular decision whether to undergo apoptosis or DNA repair is made upstream of these two processes and involves the signal transduction of the DDR (65) e.g. via PARP-1 (66) DDB2 and XPC (67). Apoptosis and DNA repair appear to be linked, in part, via the central role of cross-talk between histones to recruit repair and pro-apoptotic proteins (68) and we propose that factors associated with chromatin remodelling, or levels of binding of the above DDR elements, determine whether DNA is repaired, or apoptosis is triggered, and our evidence indicates this to be a very early event in the cellular response to UVR. Interestingly, recent evidence links PARP-1 with NER capacity and chromatin remodelling (66), together with earlier evidence of a role in signalling for apoptosis [reviewed in (69)].

The implications of this work are several-fold. Firstly, the increased cell death seen following UVB-, compared to UVA-, irradiation may have implications for the reports which examined DNA repair of CPD *in situ* in skin. Unlike in cell culture, dying and non-viable cells cannot be easily identified *in situ*, and therefore their failure to repair lesions will contribute to lesion persistence and the apparent, exaggeration of the slow rate of repair. Secondly, UVB-induced apoptosis in keratinocytes is understood to be a protective function

against skin carcinogenesis. Despite the faster repair reported here, the absence of apoptosis following UVA irradiation, represents a potential increased health risk, particularly following exposure to predominantly UVA sources, such as those in tanning booths, or certain therapeutic applications. Coupled with a report that describes UVA-induced CPD as more mutagenic than UVB (54), the absence of apoptosis would mean no backup mechanism for any cells for which repair was not entirely effective, and the potential for them to become cancerous. Finally, it is clear that there is more to determining the fate of a cell, following genotoxin exposure, than the simply the induced levels of damage. We propose that the presence or indeed persistence of the reportedly pro-apoptotic CPD is not sufficient alone to induce apoptosis, and that early changes in chromatin remodelling, following irradiation, are a more plausible trigger.

STATEMENT OF AUTHOR CONTRIBUTIONS

Drs Karbaschi, Cooke, and Evans designed the study. Drs Karbaschi, Delinassios, Abbas and Ms. Mistry ran the experiments and collected the data. Drs Karbaschi, Cooke, Evans, analysed the data and prepared draft figures and tables. Drs Karbaschi and Cooke prepared the manuscript draft with important intellectual input from Drs Evans, Macip and Young. All authors approved the final manuscript. Drs Karbaschi and Cooke had complete access to the study data.

ACKNOWLEDGEMENTS

This work was, in part, supported by funding to MSC from the Research Advisory Group of the Department of Cancer Studies and Molecular Medicine.

REFERENCES

1. Elwood JM, Jopson J. Melanoma and sun exposure: an overview of published studies. Int J Cancer. 1997;73(2):198-203.
2. Board NRP. Health Effects from Ultraviolet Radiation. Report of an advisory board on Non-ionising Radiation. 13. Didcot: NRPB; 2002.
3. Agar N, Young AR. Melanogenesis: a photoprotective response to DNA damage? Mutat Res. 2005;571(1-2):121-32.
4. Cadet J, Sage E, Douki T. Ultraviolet radiation-mediated damage to cellular DNA. Mutat Res. 2005;571(1-2):3-17.
5. Pfeifer GP, You YH, Besaratinia A. Mutations induced by ultraviolet light. Mutat Res. 2005;571(1-2):19-31.
6. Gasparro FP. Sunscreens, skin photobiology, and skin cancer: the need for UVA protection and evaluation of efficacy. Environ Health Perspect. 2000;108 Suppl 1:71-8.
7. Kvam E, Tyrrell RM. Induction of oxidative DNA base damage in human skin cells by UV and near visible radiation. Carcinogenesis. 1997;18(12):2379-84.
8. Evans MD, Cooke MS. Factors contributing to the outcome of oxidative damage to nucleic acids. Bioessays. 2004;26(5):533-42.
9. Sage E, Lamolet B, Brulay E, Moustacchi E, Chteauneuf A, Drobetsky EA. Mutagenic specificity of solar UV light in nucleotide excision repair-deficient rodent cells. Proc Natl Acad Sci U S A. 1996;93(1):176-80.
10. Kappes UP, Luo D, Potter M, Schulmeister K, Runger TM. Short- and long-wave UV light (UVB and UVA) induce similar mutations in human skin cells. J Invest Dermatol. 2006;126(3):667-75.
11. Halliday GM. Inflammation, gene mutation and photoimmunosuppression in response to UVR-induced oxidative damage contributes to photocarcinogenesis. Mutat Res. 2005;571(1-2):107-20.
12. Mouret S, Baudouin C, Charveron M, Favier A, Cadet J, Douki T. Cyclobutane pyrimidine dimers are predominant DNA lesions in whole human skin exposed to UVA radiation. Proc Natl Acad Sci U S A. 2006;103(37):13765-70.
13. Douki T, Reynaud-Angelin A, Cadet J, Sage E. Bipyrimidine photoproducts rather than oxidative lesions are the main type of DNA damage involved in the genotoxic effect of solar UVA radiation. Biochemistry. 2003;42(30):9221-6.
14. Courdavault S, Baudouin C, Charveron M, Favier A, Cadet J, Douki T. Larger yield of cyclobutane dimers than 8-oxo-7,8-dihydroguanine in the DNA of UVA-irradiated human skin cells. Mutat Res. 2004;556(1-2):135-42.
15. Rochette PJ, Therrien JP, Drouin R, Perdiz D, Bastien N, Drobetsky EA, et al. UVA-induced cyclobutane pyrimidine dimers form predominantly at thymine-thymine dipyrimidines and correlate with the mutation spectrum in rodent cells. Nucleic Acids Res. 2003;31(11):2786-94.
16. Tewari A, Sarkany RP, Young AR. UVA1 induces cyclobutane pyrimidine dimers but not 6-4 photoproducts in human skin in vivo. J Invest Dermatol. 2012;132(2):394-400.
17. Tyrrell RM. Induction of pyrimidine dimers in bacterial DNA by 365 nm radiation. Photochem Photobiol. 1973;17(1):69-73.
18. Perdiz D, Grof P, Mezzina M, Nikaido O, Moustacchi E, Sage E. Distribution and repair of bipyrimidine photoproducts in solar UV-irradiated mammalian cells. Possible role of Dewar photoproducts in solar mutagenesis. J Biol Chem. 2000;275(35):26732-42.
19. Freeman SE, Ryan SL. Wavelength dependence for UV-induced pyrimidine dimer formation in DNA of human peripheral blood lymphocytes. Mutat Res. 1990;235(3):181-6.
20. Young AR, Chadwick CA, Harrison GI, Nikaido O, Ramsden J, Potten CS. The similarity of action spectra for thymine dimers in human epidermis and erythema suggests that DNA is the chromophore for erythema. J Invest Dermatol. 1998;111(6):982-8.

21. Freeman SE, Hacham H, Gange RW, Maytum DJ, Sutherland JC, Sutherland BM. Wavelength dependence of pyrimidine dimer formation in DNA of human skin irradiated in situ with ultraviolet light. Proc Natl Acad Sci U S A. 1989;86(14):5605-9.
22. Jiang Y, Rabbi M, Kim M, Ke C, Lee W, Clark RL, et al. UVA generates pyrimidine dimers in DNA directly. Biophys J. 2009;96(3):1151-8.
23. Mouret S, Philippe C, Gracia-Chantegrel J, Banyasz A, Karpati S, Markovitsi D, et al. UVA-induced cyclobutane pyrimidine dimers in DNA: a direct photochemical mechanism? Org Biomol Chem.8(7):1706-11.
24. Sancar A. DNA repair in humans. Annu Rev Genet. 1995;29:69-105.
25. Galloway AM, Liuzzi M, Paterson MC. Metabolic processing of cyclobutyl pyrimidine dimers and (6-4) photoproducts in UV-treated human cells. Evidence for distinct excision-repair pathways. J Biol Chem. 1994;269(2):974-80.
26. de Laat WL, Jaspers NG, Hoeijmakers JH. Molecular mechanism of nucleotide excision repair. Genes Dev. 1999;13(7):768-85.
27. Hoeijmakers JH. Genome maintenance mechanisms for preventing cancer. Nature. 2001;411(6835):366-74.
28. Svejstrup JQ. Transcription repair coupling factor: a very pushy enzyme. Mol Cell. 2002;9(6):1151-2.
29. Thomas DC, Okumoto DS, Sancar A, Bohr VA. Preferential DNA repair of (6-4) photoproducts in the dihydrofolate reductase gene of Chinese hamster ovary cells. J Biol Chem. 1989;264(30):18005-10.
30. Vreeswijk MP, van Hoffen A, Westland BE, Vrieling H, van Zeeland AA, Mullenders LH. Analysis of repair of cyclobutane pyrimidine dimers and pyrimidine 6-4 pyrimidone photoproducts in transcriptionally active and inactive genes in Chinese hamster cells. J Biol Chem. 1994;269(50):31858-63.
31. van der Wees CG, Vreeswijk MP, Persoon M, van der Laarse A, van Zeeland AA, Mullenders LH. Deficient global genome repair of UV-induced cyclobutane pyrimidine dimers in terminally differentiated myocytes and proliferating fibroblasts from the rat heart. DNA Repair (Amst). 2003;2(12):1297-308.
32. Szymkowski DE, Lawrence CW, Wood RD. Repair by human cell extracts of single (6-4) and cyclobutane thymine-thymine photoproducts in DNA. Proc Natl Acad Sci U S A. 1993;90(21):9823-7.
33. Besaratinia A, Kim SI, Pfeifer GP. Rapid repair of UVA-induced oxidized purines and persistence of UVB-induced dipyrimidine lesions determine the mutagenicity of sunlight in mouse cells. FASEB J. 2008.
34. Mouret S, Charveron M, Favier A, Cadet J, Douki T. Differential repair of UVB-induced cyclobutane pyrimidine dimers in cultured human skin cells and whole human skin. DNA Repair (Amst). 2008;7(5):704-12.
35. Courdavault S, Baudouin C, Charveron M, Canguilhem B, Favier A, Cadet J, et al. Repair of the three main types of bipyrimidine DNA photoproducts in human keratinocytes exposed to UVB and UVA radiations. DNA Repair (Amst). 2005;4(7):836-44.
36. Boukamp P, Petrussevska RT, Breitkreutz D, Hornung J, Markham A, Fusenig NE. Normal keratinization in a spontaneously immortalized aneuploid human keratinocyte cell line. J Cell Biol. 1988;106(3):761-71.
37. Cooke MS, Duarte TL, Cooper D, Chen J, Nandagopal S, Evans MD. Combination of azathioprine and UVA irradiation is a major source of cellular 8-oxo-7,8-dihydro-2'-deoxyguanosine. DNA Repair (Amst). 2008;7(12):1982-9.
38. Dizdaroglu M, Zastawny TH, Carmical JR, Lloyd RS. A novel DNA N-glycosylase activity of E. coli T4 endonuclease V that excises 4,6-diamino-5-formamidopyrimidine from DNA, a UV-radiation- and hydroxyl radical-induced product of adenine. Mutat Res. 1996;362(1):1-8.

39. Doetsch PW, Zasatawny TH, Martin AM, Dizdaroglu M. Monomeric base damage products from adenine, guanine, and thymine induced by exposure of DNA to ultraviolet radiation. Biochemistry. 1995;34(3):737-42.
40. Duarte TL, Almeida GM, Jones GD. Investigation of the role of extracellular H2O2 and transition metal ions in the genotoxic action of ascorbic acid in cell culture models. Toxicology letters. 2007;170(1):57-65.
41. Dherin C, Radicella JP, Dizdaroglu M, Boiteux S. Excision of oxidatively damaged DNA bases by the human alpha-hOgg1 protein and the polymorphic alpha-hOgg1(Ser326Cys) protein which is frequently found in human populations. Nucleic Acids Res. 1999;27(20):4001-7.
42. Krishnamurthy N, Haraguchi K, Greenberg MM, David SS. Efficient removal of formamidopyrimidines by 8-oxoguanine glycosylases. Biochemistry. 2008;47(3):1043-50.
43. Dizdaroglu M, Laval J, Boiteux S. Substrate specificity of the Escherichia coli endonuclease III: excision of thymine- and cytosine-derived lesions in DNA produced by radiation-generated free radicals. Biochemistry. 1993;32(45):12105-11.
44. Dizdaroglu M, Bauche C, Rodriguez H, Laval J. Novel substrates of Escherichia coli nth protein and its kinetics for excision of modified bases from DNA damaged by free radicals. Biochemistry. 2000;39(18):5586-92.
45. Karbaschi M, Cooke MS. Novel method for the high-throughput processing of slides for the comet assay. Scientific reports. 2014;4:7200.
46. Rozen S, Skaletsky HJ. Nioinformatics Methods and Protocols: Methods in Molecular Biology. New York: Springer-Verlag; 1999.
47. Duarte TL, Cooke MS, Jones GD. Gene expression profiling reveals new protective roles for vitamin C in human skin cells. Free Radic Biol Med. 2009;46(1):78-87.
48. Pfaffl MW. Relative quantification. In: Dorak MT, editor. Real-time PCR. Abingdon: Taylor & Francis; 2008. p. 63-82.
49. Cadet J, Bourdat AG, D'Ham C, Duarte V, Gasparutto D, Romieu A, et al. Oxidative base damage to DNA: specificity of base excision repair enzymes. Mutat Res. 2000;462(2-3):121-8.
50. Hemminki K, Xu G, Kause L, Koulu LM, Zhao C, Jansen CT. Demonstration of UV-dimers in human skin DNA in situ 3 weeks after exposure. Carcinogenesis. 2002;23(4):605-9.
51. Young AR, Chadwick CA, Harrison GI, Hawk JL, Nikaido O, Potten CS. The in situ repair kinetics of epidermal thymine dimers and 6-4 photoproducts in human skin types I and II. J Invest Dermatol. 1996;106(6):1307-13.
52. D'Errico M, Lemma T, Calcagnile A, Proietti De Santis L, Dogliotti E. Cell type and DNA damage specific response of human skin cells to environmental agents. Mutat Res. 2007;614(1-2):37-47.
53. He YY, Pi J, Huang JL, Diwan BA, Waalkes MP, Chignell CF. Chronic UVA irradiation of human HaCaT keratinocytes induces malignant transformation associated with acquired apoptotic resistance. Oncogene. 2006;25(26):3680-8.
54. Runger TM, Farahvash B, Hatvani Z, Rees A. Comparison of DNA damage responses following equimutagenic doses of UVA and UVB: a less effective cell cycle arrest with UVA may render UVA-induced pyrimidine dimers more mutagenic than UVB-induced ones. Photochem Photobiol Sci. 2012;11(1):207-15.
55. Bykov VJ, Sheehan JM, Hemminki K, Young AR. In situ repair of cyclobutane pyrimidine dimers and 6-4 photoproducts in human skin exposed to solar simulating radiation. J Invest Dermatol. 1999;112(3):326-31.
56. Xu G, Snellman E, Jansen CT, Hemminki K. Levels and repair of cyclobutane pyrimidine dimers and 6-4 photoproducts in skin of sporadic basal cell carcinoma patients. J Invest Dermatol. 2000;115(1):95-9.
57. Segerback D, Strozyk M, Snellman E, Hemminki K. Repair of UV dimers in skin DNA of patients with basal cell carcinoma. Cancer Epidemiol Biomarkers Prev. 2008;17(9):2388-92.

58. Xu G, Snellman E, Bykov VJ, Jansen CT, Hemminki K. Cutaneous melanoma patients have normal repair kinetics of ultraviolet-induced DNA repair in skin in situ. J Invest Dermatol. 2000;114(4):628-31.
59. Zhao C, Snellman E, Jansen CT, Hemminki K. In situ repair of cyclobutane pyrimidine dimers in skin and melanocytic nevi of cutaneous melanoma patients. Int J Cancer. 2002;98(3):331-4.
60. Vreeswijk MP, Westland BE, Hess MT, Naegeli H, Vrieling H, van Zeeland AA, et al. Impairment of nucleotide excision repair by apoptosis in UV-irradiated mouse cells. Cancer Res. 1998;58(9):1978-85.
61. Chigancas V, Miyaji EN, Muotri AR, de Fatima Jacysyn J, Amarante-Mendes GP, Yasui A, et al. Photorepair prevents ultraviolet-induced apoptosis in human cells expressing the marsupial photolyase gene. Cancer Res. 2000;60(9):2458-63.
62. Nishigaki R, Mitani H, Shima A. Evasion of UVC-induced apoptosis by photorepair of cyclobutane pyrimidine dimers. Experimental cell research. 1998;244(1):43-53.
63. Batista LF, Kaina B, Meneghini R, Menck CF. How DNA lesions are turned into powerful killing structures: insights from UV-induced apoptosis. Mutat Res. 2009;681(2-3):197-208.
64. Orren DK, Petersen LN, Bohr VA. Persistent DNA damage inhibits S-phase and G2 progression, and results in apoptosis. Molecular biology of the cell. 1997;8(6):1129-42.
65. Nakanishi M, Niida H, Murakami H, Shimada M. DNA damage responses in skin biology--implications in tumor prevention and aging acceleration. J Dermatol Sci. 2009;56(2):76-81.
66. Robu M, Shah RG, Petitclerc N, Brind'Amour J, Kandan-Kulangara F, Shah GM. Role of poly(ADP-ribose) polymerase-1 in the removal of UV-induced DNA lesions by nucleotide excision repair. Proc Natl Acad Sci U S A. 2013;110(5):1658-63.
67. Ray A, Milum K, Battu A, Wani G, Wani AA. NER initiation factors, DDB2 and XPC, regulate UV radiation response by recruiting ATR and ATM kinases to DNA damage sites. DNA Repair (Amst). 2013;12(4):273-83.
68. Farrell AW, Halliday GM, Lyons JG. Chromatin Structure Following UV-Induced DNA Damage-Repair or Death? International journal of molecular sciences. 2011;12(11):8063-85.
69. Bouchard VJ, Rouleau M, Poirier GG. PARP-1, a determinant of cell survival in response to DNA damage. Experimental hematology. 2003;31(6):446-54.

Fig 1 Spectral analysis of (A) Cleo performance lamps through M-UG2 glass filter, and (B) TL01 lamps.

A

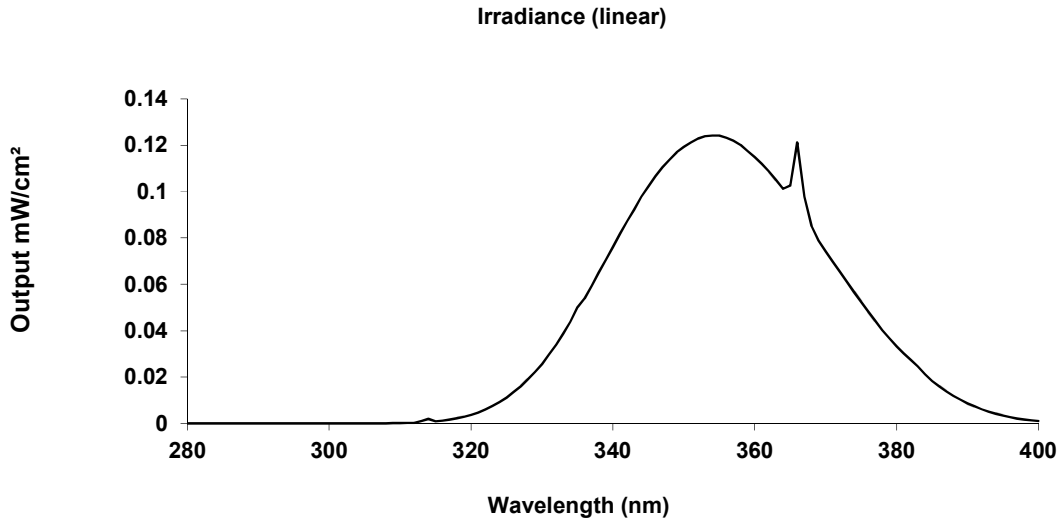

B

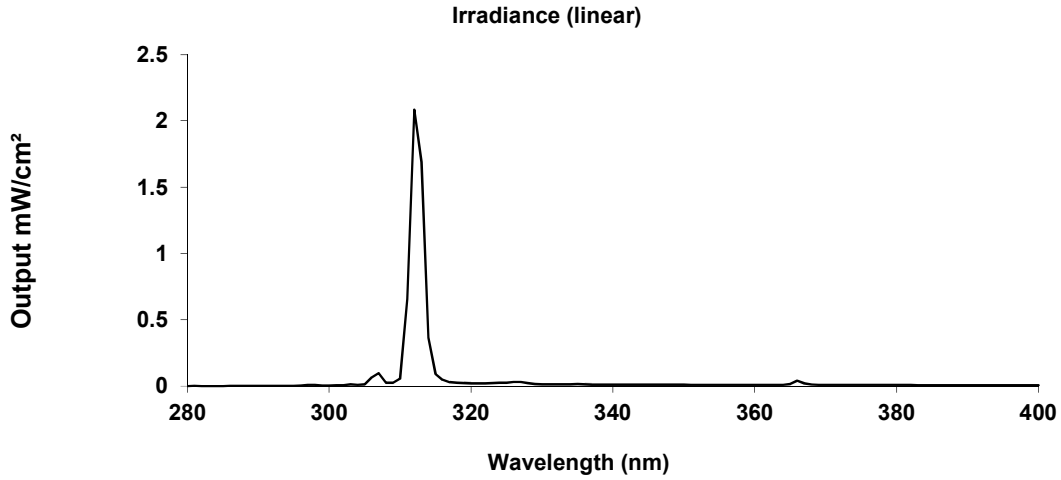

Fig 2 Induction of CPD (+T4endoV) and SSB/ALS (-T4endoV) in HaCaTs following irradiation with (A) 10 J/cm^2 UVA, or (B) 1 J/cm^2 UVB, determined by T4endoV-modified comet assay immediately after irradiation. Control, sham irradiated (CSI) samples were not irradiated. Error bars represent for mean + SEM of 300 individual determinations, from three independent experiments.

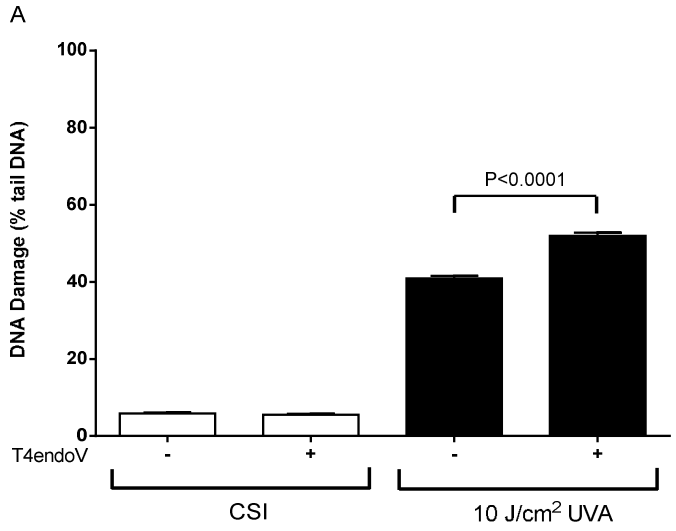

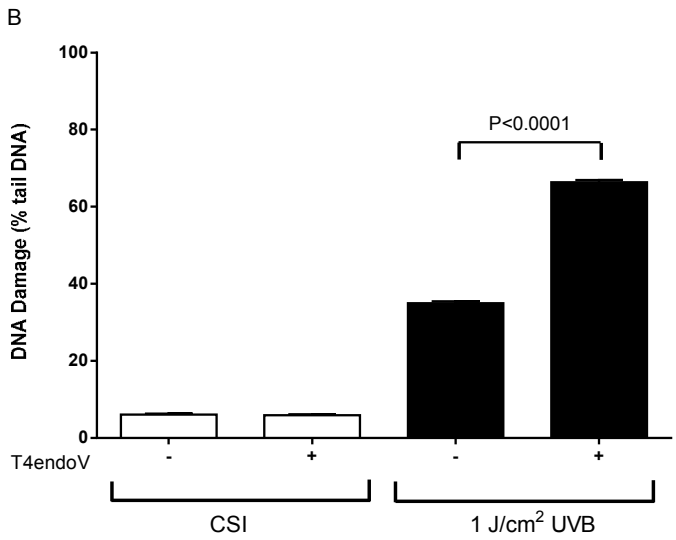

Fig 3 Repair kinetics of UVA- and UVB-induced CPD repair in (A) HaCaTs, and (B) HDFs, determined by T4endoV-modified comet assay. Cells were irradiated with 10 J/cm^2 UVA or 1 J/cm^2 UVB. *** represents P<0.0001 comparing UVA treated vs. UVB treated cells. Fig. 2A (inset) represents repair kinetics of UVA- and UVB-induced CPD in HaCaTs over the first one hour post-irradiation. Error bars represent mean +/- SEM of 300 individual determinations, from three independent experiments. Figure 3 C illustrates the dose-response for UVB-induced CPD, determined by T4endoV-modified comet assay, for doses used in Fig. 2D. Fig. 2D represents the kinetics of CPD repair, with increasing UVB dose; 200 individual comets from two independent experiments were scored to generate each mean data point.

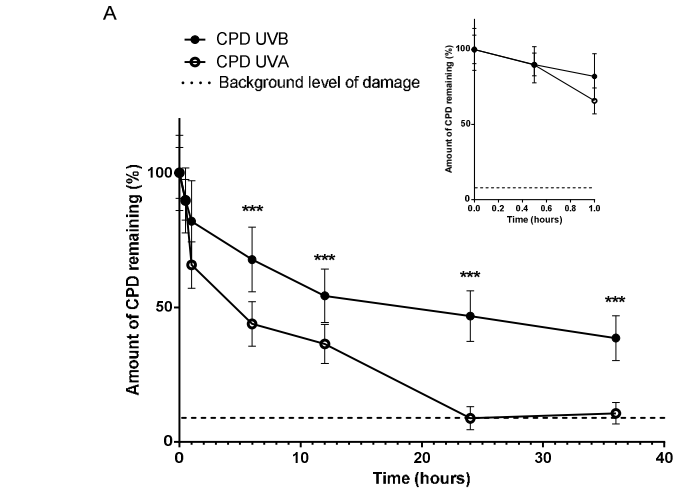

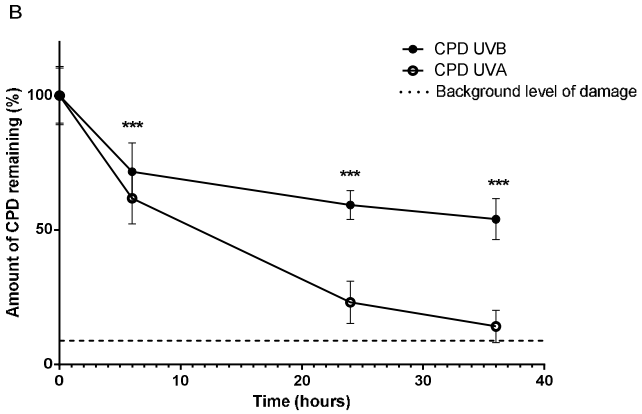

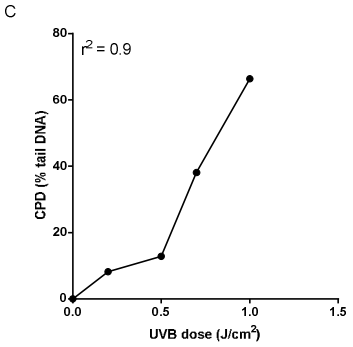

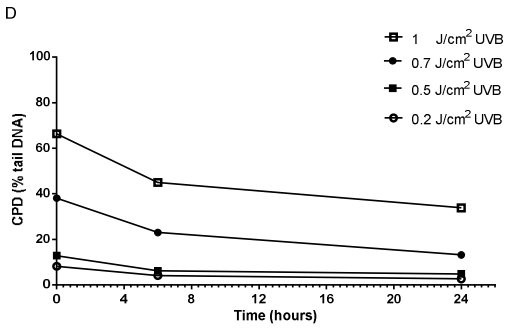

Fig 4 Induction of CPD (+T4endoV) and SSB/ALS (-T4endoV) in HDFs following irradiation with (A) 10 J/cm^2 UVA, or (B) 1 J/cm^2 UVB, determined by T4endoV-modified comet assay, immediately after irradiation. Control, sham irradiated (CSI) samples were not irradiated. Error bars represent for mean + SEM of 300 individual determinations from three independent experiments. Repair kinetics of UVA- and UVB-induced SSB/ALS repair in (C) HaCaTs, and (D) HDFs, determined by alkaline comet assay. Cells were irradiated with 10 J/cm^2 UVA or 1 J/cm^2 UVB. Error bars represent for mean + or +/- SD of 300 individual determinations from three independent experiments.

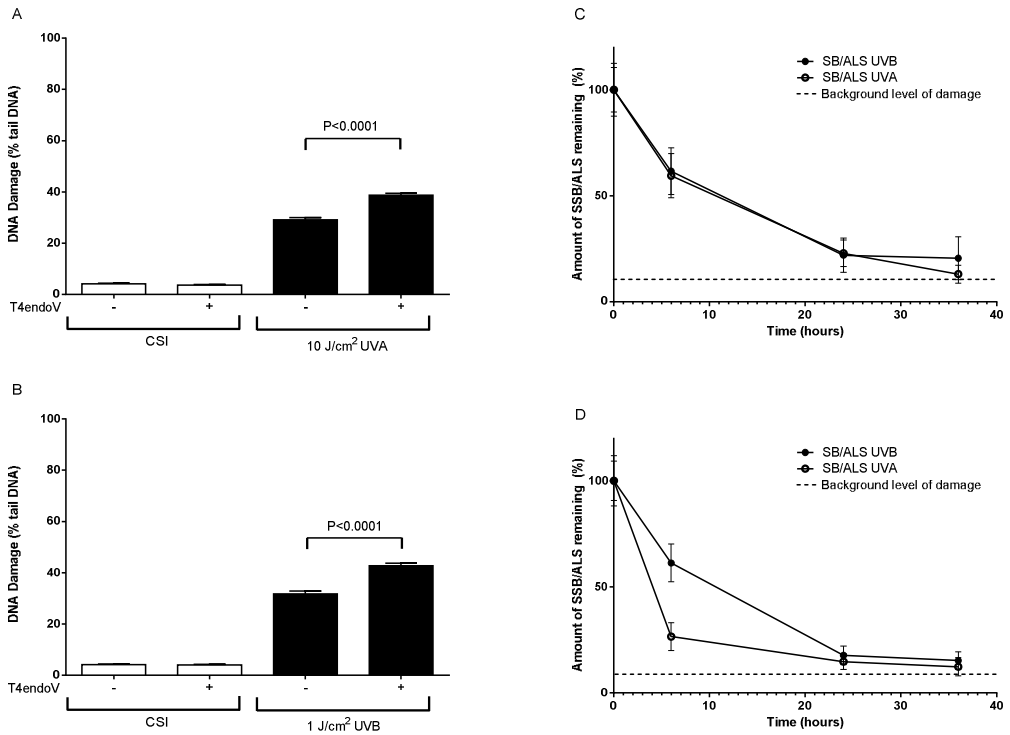

FIG 5 (A) Induction of oxidised purines[§] (+hOGG1), predominantly 8-oxoGua, and SB/ALS (-hOGG1) in HaCaTs following irradiation with 10 J/cm^2 UVA, or 1 J/cm^2 UVB, determined by hOGG1-modified comet assay. Control, sham irradiated (CSI) samples were not irradiated. Error bars represent mean + SEM of 300 individual determinations, from three independent experiments. Repair kinetics of UVA- and UVB-induced oxidised purines in (B) HaCaTs, and (C) HDFs, determined by hOGG1-modified comet assay. Cells were irradiated with 10 J/cm^2 UVA or 1 J/cm^2 UVB. Error bars represent mean +/- SD of 300 individual determinations, from three independent experiments. *** represents $P<0.0001$ comparing UVA treated vs. UVB treated cells. (D) Repair kinetics of oxidised purines and oxidised pyrimidines[§] in HaCaTs, determined by hOGG1- and endoIII-modified comet assay, respectively, following exposure to 100 μM H_2O_2 for 30 min. Error bars represent mean + or +/- SD of 300 individual determinations, from three independent experiments

[§] Oxidised purines is a general term to describe the oxidatively generated nucleobase products recognized by hOGG1. We note that although the formation of FapyGua and FapyAde are ultimately reduction products, their formation is initiated by an oxidation step. Similarly oxidised pyrimidines is a general term to describe the oxidatively generated nucleobases products recognized by endoIII, which are exclusively pyrimidine-derived, with the exception of FapyAde.

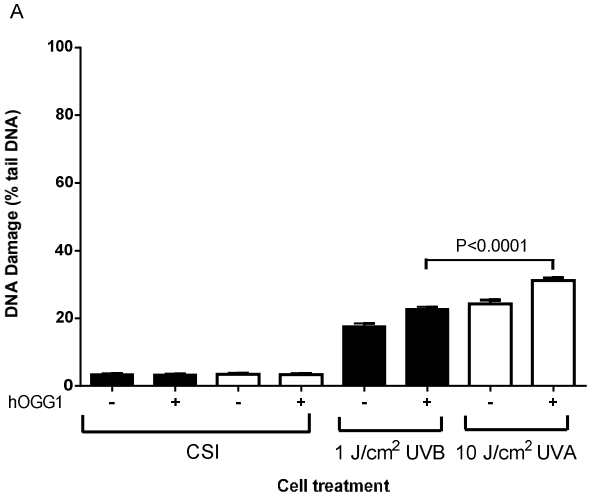

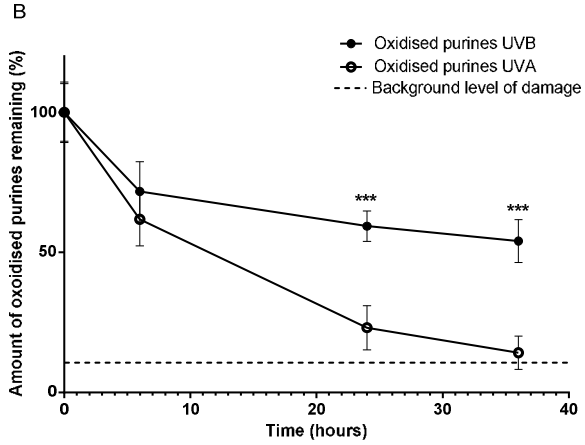

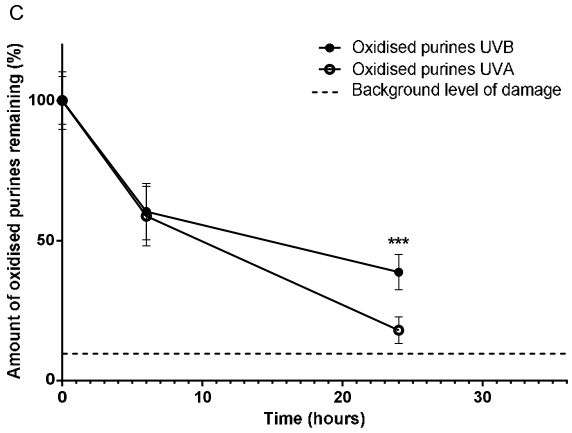

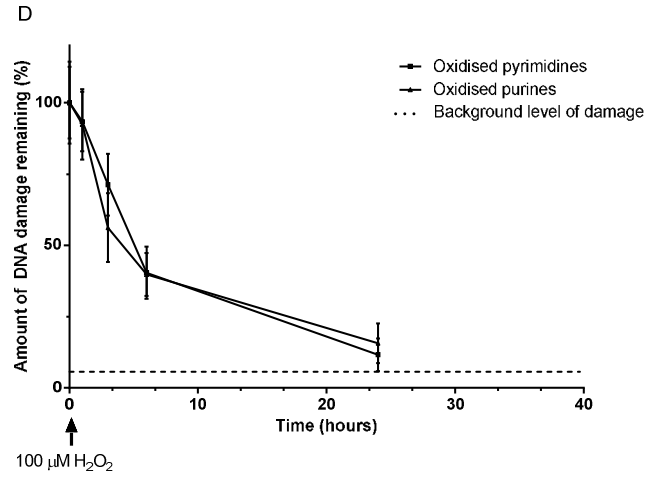

FIG 6 Cell viability, determined by flow cytometry, and gene expression analysis. HaCaTs were irradiated with (A) 10 J/cm^2 UVA or (B) 1 J/cm^2 UVB, and HDFs were irradiated with (C) 10 J/cm^2 UVA or (D) 1 J/cm^2 UVB, and then allowed to repair. At time points indicated, cells were stained with Annexin V and propidium iodide and analysed with Cell Quest software. Control sham irradiated (CSI) samples were not irradiated. (E) Post-irradiation changes in the expression of three key genes involved in NER (XPA, XPC and ERCC1, normalised to the expression of GAPDH), determined by qPCR in HaCaTs treated as in (A) and (B). Results represent the mean of (+ SD) of two independent experiments

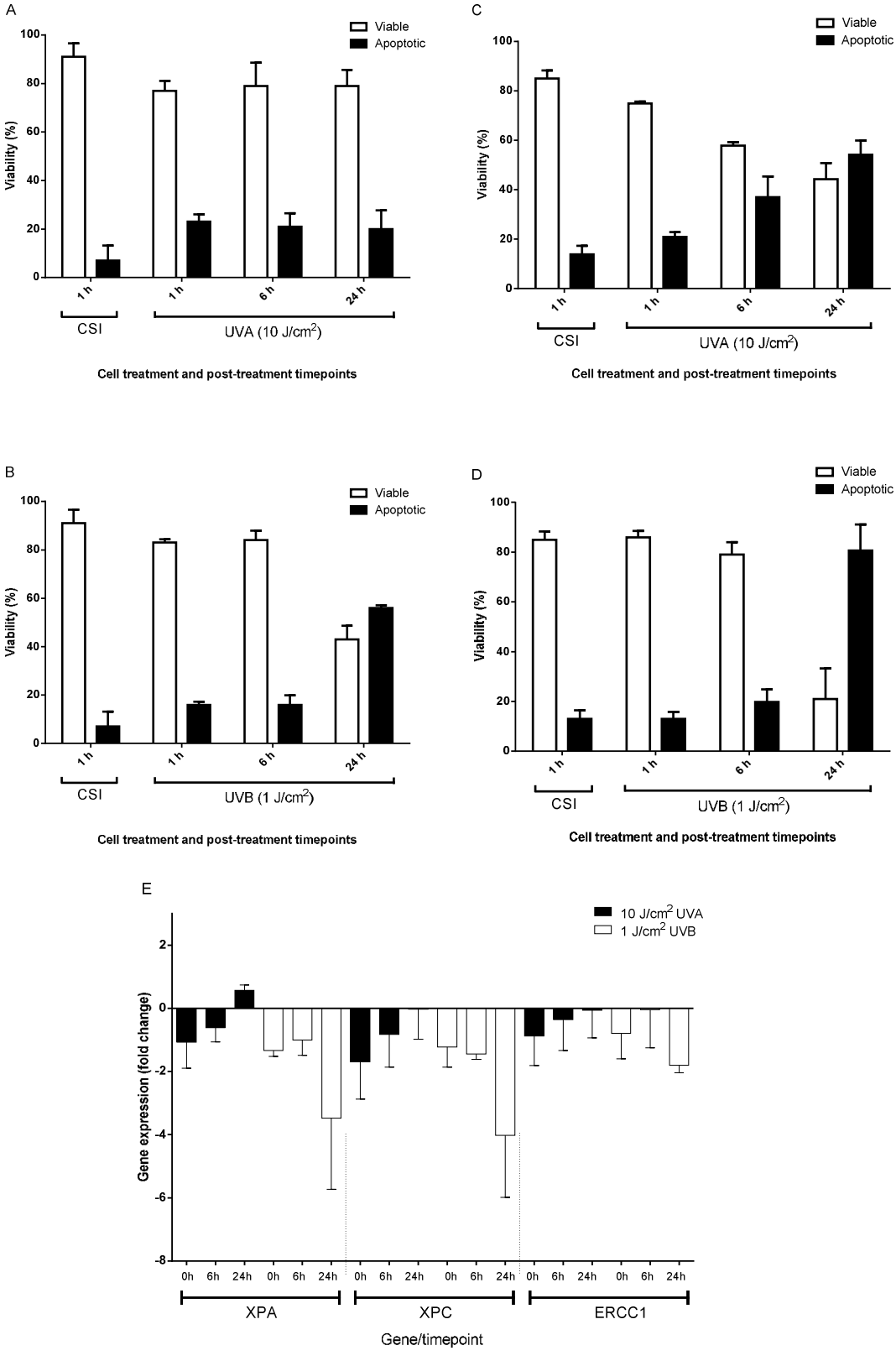

FIG 7 (A) Effect of Z-VAD-FMK concentration on CPD repair in HaCaT. Cells were incubated with Z-VAD-FMK (0-300 μM) for 24 h prior, exposure to 1 J/cm^2 UVB. After a period of 24 h, to allow for potential DNA repair, cells were then analysed for CPD (+T4endoV) by T4endoV-modified comet assay. Each bar indicates mean + SEM for 200 determinations, n=2 experiments. (B) Representative Western blot analysis of protein extract performed as described for (A), showing effect of Z-VAM-FMK treatment upon protein expression. Indicated on the figure is the position of the 17-kDa cleaved caspase 3 band. (C) Cell viability, determined by flow cytometry with Annexin V and propidium iodide staining and analysis with Cell Quest software, for two experiments performed as described in (A). Each bar indicates mean + SEM